

Kinematic Reductions for Uncertain Mechanical Contact

Todd D. Murphey

Abstract

This paper describes methods applicable to the modeling and control of mechanical contact, particularly those systems that experience uncertain stick/slip phenomena. Geometric kinematic reductions are used to reduce a system's description from a second-order dynamic model with frictional disturbances coming from a function space to a first-order model with frictional disturbances coming from a space of finite automata over a finite set. As a result, modeling for purposes of control is made more straight-forward by getting rid of some dependencies on low-level mechanics (in particular, the details of friction modeling). Moreover, the online estimation of the uncertain, discrete-valued variables has reduced sensing requirements. The primary contributions of this paper are the introduction of a simplifying representation of friction and formal tests for kinematic reducibility. Results are illustrated using a slip-steered vehicle model and an actuator array model.

1 Introduction

It is traditional in robotics to view problems of manipulation, motion planning, and control in one of two extreme lights. First, if a system is kinematic, the system description is simplified from a second-order system with forces and inertias to a first-order system that consists of velocities and constraints. Then motion plans and control laws (if necessary) are designed for this kinematic system. It is important to note that in order to *implement* this plan based on kinematics, a backstepping algorithm is employed, either explicitly in an “inner-loop-outer-loop” control architecture, or implicitly by purchasing motor controllers (or other appropriate devices) that provide the inner loop control. In the end, the advantages of using kinematic structures include both lessened computational burden (due to the computation in a lower-dimensional space) and increased robustness to some classes of uncertainty (due to robustness properties of the backstepping, inner-loop controller).

If, however, there is some reason that a kinematic analysis is inappropriate, then one often reverts to a more complex set of modeling choices. In particular, in multi-point contact many phenomena are introduced, including soft-contact models [2], elaborate models of frictional interfaces [20], and the inclusion of dynamic effects such as inertial terms and generalized forces. Nevertheless, it is not clear that the introduction of these additional modeling techniques helps for the purpose of control, motion planning, etcetera. In particular, the task description typically does not include these effects, so one should only incorporate them in the representation in use for planning and control if they are actually necessary for task completion (which they typically are not). In fact, it is often the case that the inclusion of these details *hurts* our ability to successfully design control strategies. Not only does the introduction of these effects make problems computationally more complex, it also decreases robustness by introducing assumptions that are often not satisfied by the environment or, worse, may only sometimes be satisfied by the environment. Hence, one can be faced with a situation where our modeling assumptions are occasionally correct, but not reliably so.

From a design perspective (as opposed to a simulation perspective), it is thus desirable to, if necessary, introduce elements to a model that provide the full complexity of possible behavior of the system without introducing too much new information (thereby decreasing the applicability of the model).

This paper shows how notions of kinematic reducibility can allow one to recast a dynamic system that has frictional effects belonging to a function space into a first-order system that has frictional effects that form a finite automaton over a finite set. Hence, the goal of the reduction is *not* solely or even primarily to reduce from a second-order equation to a first-order equation. (Cutting a search space in half is not particularly beneficial from a computational perspective, and would not motivate all the formality.) Rather, the thing of interest is the induced mapping from the function space of friction laws over a vector space to the space of finite automata over the finite set of contact states. This provides a representation of friction that is simultaneously more simple and less naive (in the sense that one no longer needs to know *which* friction law is governing the dynamic equations of motion for purposes of implementation).

Two examples are discussed in-depth to illustrate the broad applicability of the framework—a slip-steered vehicle in Section 6.1 and actuator arrays in Section 6.1. Surprisingly, slip-steered vehicles are almost always kinematic, but their dynamic states should be avoided to avoid having to calculate motion plans in the full space. Moreover, orthogonal actuator arrays are *always* kinematic. This is true even if all contact points are slipping against the surface of a manipulated object, so long as the frictional interaction is strictly dissipative.

This paper is organized as follows. Section 2 describes two overconstrained example systems that motivate the present work and that will be used as examples later in Section 6. Section 3 discusses modeling of multi-point contact systems using the constrained affine connection and introduces a new way of representing friction that is amenable to kinematic analysis. Section 4 contains the other main results of the paper on kinematic reduction for systems with external forces. Because control and estimation are occurring directly in the reduced space, Section 5 discusses the method employed for estimating discrete variables, in this case the contact state of the system. Section 6 discusses a slip-steered vehicle and actuator arrays from Section 2.

2 Motivation: Mechanical Contact Systems

A system consisting of many points of contact typically exhibits stick/slip phenomenon due to the point contacts moving in kinematically incompatible manners. This manner of motion is called *overconstrained motion* because not all of the constraints can be satisfied.

Consider the first example in Fig. 1. Scratch drive actuators (SDA) are characterized by being able to produce large deflections (on the order of $500\ \mu\text{m}$), relatively large forces (on the order of $100\ \mu\text{N}$), with high precision step sizes (on the order of $30\ \text{nm}$). They can be arrayed on chips with as few as ten SDA actuators on a chip. Despite the fact that these devices were first developed over ten years ago [1], only recently has any formal work been done on modeling and control for these devices [13].

Modeling these devices depends heavily on the particulars of the brushing geometry, plate thickness, insulator properties, and the plate Young's modulus. However, an in-depth analysis of such a device was performed in [13]. The main important result of that analysis is that one can drive the actuators at a desired velocity, despite considerable uncertainty in the force characteristics. Hence, SDAs are most naturally described in terms of kinematic relationships, at least when considered individually. Solving for the forces is difficult here as well, as at the micro-scale they are typically not well defined using traditional friction models. Hence, it is desirable for any control strategy to not require this modeling and to take advantage of being able to reliably drive these actuators at a desired velocity.

Consider the vehicle object in Fig. 2. It has four independently driven wheels, but no steering capability. Hence, its wheels must slip sideways in order to turn. Because this vehicle will typically be outdoors in an unstructured environment, there is no reason to believe that any particular friction model

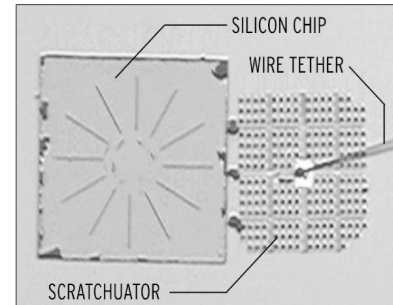


Figure 1: Scratch Drive Actuators (SDA) (Figures taken from [13]). SDAs are chips covered with a large number of actuators along with the gold tether that is used to send voltages down to the SDAs. Despite being able to drive SDA actuators quite reliably, the individual forces are difficult to model accurately.

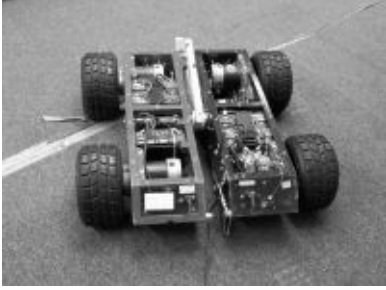


Figure 2: The “Flexy-Flyer” slip-steered vehicle in the author’s laboratory <http://robotics.colorado.edu>. In order to turn, the vehicle must violate sideways-slip constraints.

will capture the details of the dynamics. Moreover, even if one *could* describe the friction model properly, online system identification would be necessary, which requires high-bandwidth calculations. Both this example and the previous example are discussed in detail in Section 6, where it will be illustrated that much lower bandwidth sensing is possible if calculations are performed using the kinematic equations of motion.

3 Modeling and Analysis of Multiple Point Contact

The systems considered here are finite-dimensional simple mechanical systems (as described for smooth systems in [5]). That is, their equations of motion may be found using a Lagrangian of the form kinetic energy minus potential energy ($L = K.E. - V$) along with a set of constraints on the system of the form $\omega(q)\dot{q} = 0$, where $\omega(q)$ is a matrix representing the configuration q dependent constraints. Moreover, there may be external forces acting on the system. If one ignores potential energy (as is appropriate for many planar systems including the ones described in Section 2), such a system’s dynamics may be represented as:

$$\nabla_{\dot{q}}\dot{q} = u^\alpha Y_\alpha, \tag{1}$$

where the notation $u^\alpha Y_\alpha$ implies summation over the α . In this expression, ∇ is the constrained affine connection encoding the free kinetic energy and any constraints on the system. Moreover, $u \in \mathcal{U}_{\text{input}}$ ($u : [0, T] \rightarrow \mathbb{R}^m$) represents external forces (not necessarily inputs) where $\mathcal{U}_{\text{input}}$ is the space of essentially-bounded, Lebesgue-integrable external forces [6]. The Y terms represent the associated vector fields on the configuration manifold Q (i.e., $Y \in T_q Q$, the tangent space at $q \in Q$). If one wishes to include potential energy, it will show up as a vector field on the right-hand side of the equation. A short description of this formulation of mechanics may be found in the Appendix.

The systems of interest have two types of external forces—those that correspond to inputs and those

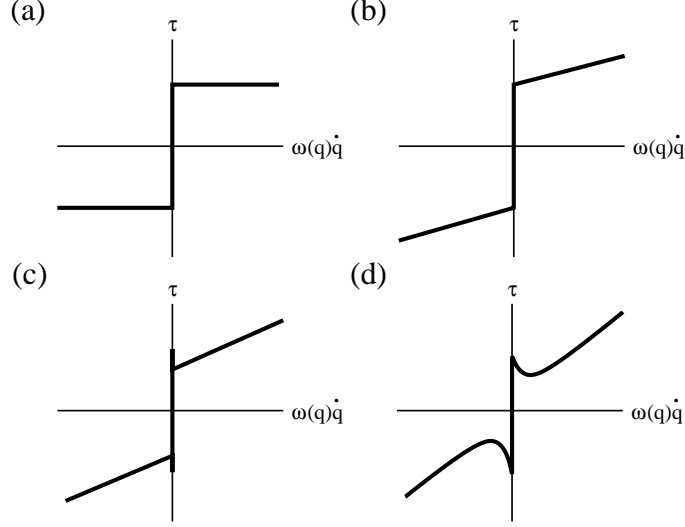


Figure 3: Types of friction model, including (a) Coulomb friction, (b) Coulomb plus viscous friction, (c) Coulomb/viscous stiction, and (d) Nonlinear smoothing of stiction.

that correspond to external disturbances. In the case of multiple point contact, the external disturbance forces ($d \in \mathcal{U}_{\text{disturbance}}$ where $d : [0, T] \rightarrow \mathbb{R}^l$ and where $\mathcal{U}_{\text{disturbance}}$ is also a space of essentially-bounded, Lebesgue-integrable functions) generally correspond to reaction forces due to friction when a contact slips. Therefore, it will be useful to write the dynamic equations as: $\nabla_{\dot{q}} \dot{q} = u^\alpha Y_\alpha + d^\beta V_\beta$ so that a distinction between external forces that can be controlled and those that cannot can be made.

3.1 Standing Assumptions on Friction

Consider some of the standard friction models, seen in Fig. 3. These of course include Coulomb friction ($F = F_C \text{sign}(v)$ for $F_C > 0$), but additionally include viscous friction, stiction, and nonlinear versions, such as a better representation of viscous friction. These are respectively represented as

$$F = \begin{cases} F_V v + c & v > 0 \\ (-c, c) & v = 0 \\ F_V v - c & v < 0 \end{cases} \quad F = \begin{cases} F_V v + c & v > 0 \\ (-c - \delta, c + \delta) & v = 0 \\ F_V v - c & v < 0 \end{cases} \quad F = \begin{cases} F_V |v|^{\delta_c} \text{sign}(v) + c & v > 0 \\ (-c, c) & v = 0 \\ F_V |v|^{\delta_c} \text{sign}(v) - c & v < 0 \end{cases}$$

for $F_V, c, \delta > 0$. These are seen in Fig. 3. Moreover, there are many more types of friction model to choose from, including dynamic models of friction like Dahl and LuGre models [20] or even more heuristic mod-

els such as Pacejka’s “Magic Tire Formula”—each with their own specialized area of applicability. What one would like is a description of friction that does not depend on any of these particular characteristics. Although they are qualitatively similar to each other, we would like to conservatively bound the class of friction models and choose a reduction that is invariant with respect to the particular friction model.

With this goal in mind, replace the family of curves seen in Fig. 3 by the conservative estimation of those curves seen in Fig. 4. In this figure, the friction law need only be dissipative. That is, $v > 0 \Rightarrow \tau > 0$ and $v < 0 \Rightarrow \tau < 0$. If $v = 0$, then $\tau \in \mathbb{R}$ —that is, stiction (constraint) forces are allowed, and frictional constraints are allowed. (This is the first time any use for the constrained affine connection becomes apparent.) The important thing to note is that $v \neq 0 \Rightarrow \tau \neq 0$ —this will be important later. In any case, the friction curve can be any absolutely continuous curve that has all its values in the grayed regions in Fig. 4.

(Ultimately τ will be restricted slightly more for purposes of stability analysis.) Hence, if $\omega(q)\dot{q}$ is the slipping velocity at some point, we restrict τ in the following manner.

$$\tau(\omega(q)\dot{q}) = \begin{cases} \tau^+(\omega(q)\dot{q}) > 0 & \text{if } \omega(q)\dot{q} > 0 \\ \tau^-(\omega(q)\dot{q}) < 0 & \text{if } \omega(q)\dot{q} < 0 \\ \tau^0(\omega(q)\dot{q}) \in \mathbb{R} & \text{if } \omega(q)\dot{q} = 0 \end{cases} \quad (2)$$

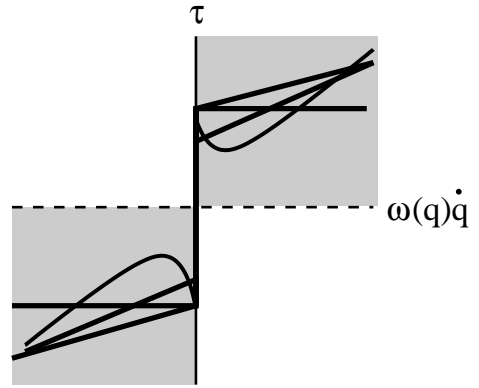


Figure 4: Friction is only assumed to be dissipative, so that any curve in the grayed areas is a valid friction model. Clearly, this includes all the friction models in Fig. 3 (shown again here) and more [20].

With this picture in mind, one can now *choose* an equivalence class on $\tau \in \mathcal{L}$ (the space of all possible absolutely continuous curves satisfying Eq. (2)) that will be familiar. In particular, let us consider the cases $\omega(q)\dot{q} = 0$ (when the system is constrained) and $\omega(q)\dot{q} \neq 0$ (when the system is sliding) separately. *That is, we arbitrarily choose to distinguish between slipping friction forces and constraint friction forces.* This canonical distinction is traditionally referred to as the *contact state* of a system. Note that there is no reason to treat these as canonically different from each other. In fact, one could argue that it is better to treat systems with frictional contact as unconstrained

systems with frictional forces determined by the force laws such as those in Fig. 3. However, distinguishing between geometrically constrained and unconstrained situations allows one to take advantage of deep geometric results regarding kinematic reducibility, which in turn take advantage of algebraic calculations using the affine connection.

In particular, when $\omega(q)\dot{q} = 0$, the dynamics may still be written as $\nabla_{\dot{q}}\dot{q} = u^\alpha Y_\alpha$, where ∇ is now the constrained affine connection and Y_α are appropriately projected onto the distribution (see Appendix). Moreover, because the contact state changes over time (as the contacts transition between stick and slip), the constraints change over time. This implies that ∇ is not a single constrained affine connection, but rather comes from a discrete set of constrained affine connections ∇^σ (indexed by $\sigma \in \Sigma$ where Σ is a finite set), each of which represents a different set of stick/slip states of the mechanism. The same holds true for Y^σ and V^σ . Hence, if one indexes the set of possible stick/slip states by σ , one gets second-order equations of motion of the following form:

$$\nabla_{\dot{q}}^\sigma \dot{q} = u^\alpha Y_\alpha^\sigma + d^\beta V_\beta^\sigma \quad (3)$$

where u are input forces and d are external forces. Moreover, σ will evolve over Σ with time according to the reaction force description. Typically the automaton that describes the evolution of σ over its potential values in Σ depends on the continuous calculation of constraint forces that enforce a constraint. If one of these forces exceeds a critical value, for instance the coefficient of stiction μ_S , then the constraint is broken and σ changes. Reducing Eq. (3) to a first-order description without friction and retaining σ as the representation of frictional effects is the focus of Section 4.

4 Kinematic Reduction With External Forces

We now focus on kinematic reductions [5–8, 12, 18]. Smooth kinematic reductions take systems of the form of Eq. (1) and convert them into systems of the form

$$\dot{q} = \bar{u}^a X_a, \quad (4)$$

where $q \in Q$, $X_a(q) \in T_qQ$, and $\bar{u} : [0, T] \rightarrow \mathbb{R}^m$. Note that the controls $\bar{u} \in \mathcal{U}_{\text{kin}}$ are now kinematic inputs (i.e., velocities, where \mathcal{U}_{kin} is the space of piecewise absolutely continuous functions) instead of generalized forces. The affine connection formalism in Section 3 is used to describe mechanical systems because it is in the context of this formalism that a useful technical connection between 2nd-order mechanical systems and 1st-order kinematic systems has been made (found for smooth systems in [12] and for nonsmooth systems in [18]). In particular, it would be useful to be able to write Eq. (3) in the form:

$$\dot{q} = \bar{u}^a X_a^\sigma, \quad (5)$$

where $\sigma \in \Sigma$ is allowed to switch the vector fields X discretely just as it does in Eq. (3). That is, we would like to perform this reduction in the presence of switching in σ and external forces d^b . Note that in the kinematic setting it is not clear that one can calculate the automaton that represents the evolution of σ because the reaction forces cannot be calculated. This leads to the need for online estimation of σ , which is discussed in Section 5.

An algebraic test for kinematic reduction relies on the *symmetric product* between two vector fields Y_i^σ and Y_j^σ for a particular σ , which is defined by $\langle Y_i^\sigma : Y_j^\sigma \rangle = \nabla_{Y_i^\sigma} Y_j^\sigma + \nabla_{Y_j^\sigma} Y_i^\sigma$ for given i, j . We will see that the algebraic test of kinematic reducibility is: the symmetric product between any two vector fields Y_i^σ and Y_j^σ must lie within the distribution of the vector fields and any reaction force vector field V_β^σ must also lie within the distribution of the input vector fields. That is, the system in Eq.(3) is kinematically reducible to the one in Eq.(5) if and only if the following conditions hold.

$$\langle Y_i^\sigma : Y_j^\sigma \rangle \in \text{span}_{\mathbb{R}}\{Y_i^\sigma | i = 1, \dots, m\} \quad \forall i, j, \sigma \quad (6)$$

$$V_\beta^\sigma \in \text{span}_{\mathbb{R}}\{Y_i^\sigma | i = 1, \dots, m\} \quad \forall \beta, \sigma \quad (7)$$

where $\text{span}_{\mathbb{R}}$ is the span over the field \mathbb{R} . This result is the focus of the rest of this section.

4.1 Reduction for single model systems

Initially reduction for single model systems of the following form is considered.

$$\nabla_{c'(t)} c'(t) = u^a(t) Y_a(c(t)) + d^b(t) V_b(c(t)) \quad (8)$$

In this equation ∇ is the (possibly constrained) affine connection associated with the Riemannian metric G , d^b belongs to a family of disturbance signals \mathcal{D} that take values in $U_{\text{disturbance}}$ and meet the assumptions in Section 3.1 in Eq. (2), V_b is the set of corresponding vector fields, u^a belongs to a family of control input signals \mathcal{U} taking values in U_{input} , and Y_a are the associated vector fields. Since the motivation here is not wanting to be forced to rely on the correctness of one particular disturbance force model (such as friction force modeling where there are many possible choices of model), the term d^b is presumed to be set-valued for each index b , as in Fig. 4. If d^b as a set is not convex, then it is replaced by its convex hull $\text{co}\{d^b\}$ so as to guarantee solutions exist in the Filippov sense [9].

Now, given a system with set-valued disturbances such as in Eq. (8), under what circumstances it can be reduced to a system of the form in Eq. (1)? That is, when can one find an equivalent system that does not include external disturbance forces. To make such an equivalence more rigorous, we introduce some definitions, following the Appendix for guidance. In particular, we use the notion of a $(\mathcal{U}, \mathcal{D}, \mathcal{T})$ -solution (a trajectory given signals coming from a family of controls \mathcal{U} and from a family of disturbances \mathcal{D}), $(\mathcal{U}, \mathcal{D})$ -reducible (reduction from $(\mathcal{U}, \mathcal{D}, \mathcal{T})$ -solution to $(\mathcal{U}, \mathcal{T})$ -solutions), and $((\mathcal{U}, \mathcal{D}), \bar{\mathcal{U}})$ -reducible (reduction from $(\mathcal{U}, \mathcal{D}, \mathcal{T})$ -solutions to $(\bar{\mathcal{U}}, \mathcal{T})$ -solutions, where $\bar{\mathcal{U}}$ is a new family of control inputs for the kinematic system). See the Appendix for further discussion of these definitions.

Definition 4.1 *Let Σ_s be a smooth control system $\dot{q} = f(q, u, d)$ on a smooth manifold M . A $(\mathcal{U}, \mathcal{D}, \mathcal{T})$ -solution to Σ_s is a triple (c, u, d) , where $u : [0, T] \rightarrow \mathbb{R}^m$, $d : [0, T] \rightarrow \mathbb{R}^l$, and $c : [0, T] \rightarrow M$ satisfy $c'(t) = f(c(t), u(t), d(t))$.*

(This is simply an extension of the definition of the $(\mathcal{U}, \mathcal{T})$ -solution to a smooth control system $\dot{q} = f(q, u)$ found in the Appendix.) Again using the definitions found in the Appendix for guidance, we define the following notion of reduction.

Definition 4.2 Let ∇ be an affine connection on Q , and let \mathcal{U} be a family of control functions and \mathcal{D} be a family of disturbance functions. The system in Eq. (8) is $(\mathcal{U}, \mathcal{D})$ -reducible to the system in Eq. (1) if for each $(\mathcal{U}, \mathcal{D}, \mathcal{T})$ -solution (η_1, u_1, d) of the Eq. (8) there exists a $(\mathcal{U}, \mathcal{T})$ -solution (η_2, u_2) of Eq. (1) with $\eta_1(t) = \eta_2(t)$;

Lastly, one would like to be rigorous about what it means for a mechanical system with set-valued disturbances to be reducible to a kinematic system, which leads to the following definition (based on Def. A.4).

Definition 4.3 Let ∇ be an affine connection on Q , and let \mathcal{U} and $\bar{\mathcal{U}}$ be two families of control functions. The system in Eq. (8) is $((\mathcal{U}, \mathcal{D}), \bar{\mathcal{U}})$ -reducible to the system in Eq. (4) if the following two conditions hold:

- i) for each $(\mathcal{U}, \mathcal{D}, \mathcal{T})$ -solution (η, u, d) of the dynamic Eq. (1) with initial conditions $\eta(0)$ in the distribution D_{kin} , there exists a $(\bar{\mathcal{U}}, \mathcal{T})$ -solution (γ, \bar{u}) of the kinematic Eq. (4) with the property that $\gamma = \tau_Q \circ \eta$;
- ii) for each $(\bar{\mathcal{U}}, \mathcal{T})$ -solution (γ, \bar{u}) of the kinematic Eq. (4), there exists a $(\mathcal{U}, \mathcal{D}, \mathcal{T})$ -solution (η, u, d) of the dynamic Eq. (1) with the property that $\eta(t) = \gamma'(t)$ for almost every $t \in [0, T]$.

With these definitions, we can state sufficient conditions for a system to be $(\mathcal{U}_{input}, \mathcal{U}_{disturbance})$ -reducible or $((\mathcal{U}_{input}, \mathcal{U}_{disturbance}), \mathcal{U}_{kin})$ -reducible. Intuitively, this corresponds to being able to guarantee that any solutions that include disturbances can be mapped directly to a solution that has no disturbances.

Lemma 4.1 Assume one has a mechanical system of the form in Eq. (8) with unbounded inputs and dissipative friction forces τ as in Eq.(2). Then the system in Eq. (8) is $(\mathcal{U}_{input}, \mathcal{U}_{disturbance})$ -reducible to the mechanical system in Eq. (1) iff this system satisfies $V_b \in \text{span}_{\mathbb{R}}\{Y_a\}$ for all b .

Proof: The condition is clearly necessary because if $V_b \notin \text{span}_{\mathbb{R}}\{Y_a\}$ one automatically has a trajectory that the system cannot follow just using the control inputs. Sufficiency is nearly as clear. Suppose we have a $(\mathcal{U}, \mathcal{D}, \mathcal{T})$ -solution Φ_d where $V_b \in \text{span}_{\mathbb{R}}\{Y_a\}$. We know that even if the control u^a is a function of τ it can be made any nonzero value by the assumption in Eq.(2). Hence, Φ_d can locally be represented as $\Phi_d = \lim_{n \rightarrow \infty} \left(\prod_i \Phi_{\frac{\delta_i}{n} Y_i} \right)^n(q_0)$ for some δ_i such that $\sum_i \delta_i = 1$ [18]. (Here $\Phi_{\frac{\delta_i}{n} Y_i}(q_0)$ is the flow of Eq. (1) along

Y_i for δ_i/n , \amalg represents sequential composition of mappings, and a mapping to the n^{th} power is simply composed with itself n times.) Because d^b is convex, a limit of a sequence of solutions to the differential inclusion must be a solution as well [9], so this limit is a $(\mathcal{U}, \mathcal{T})$ -solution to Eq. (1). ■

This means that all trajectories can be planned as if there are no forces due to the terms $d^b V_b$. However, it is important to note that the requirement that $u^a \neq 0$ is satisfied precisely because we do not allow $\tau \neq 0$ for $v \neq 0$. We are now interested in finding out when a multiple model of the form in Eq.(3) is reducible to a system of the form in Eq. (5).

Theorem 4.2 *Equation (3) is $((\mathcal{U}_{\text{input}}, \mathcal{U}_{\text{disturbance}}), \mathcal{U}_{\text{kin}})$ -reducible iff Equation (3) is $((\mathcal{U}_{\text{input}}, \mathcal{U}_{\text{disturbance}}), \mathcal{U}_{\text{kin}})$ -reducible for every constant σ (i.e., Eqs. (6) and (7) hold for any choice of σ).*

Proof: Suppose that Equation (3) is $((\mathcal{U}, \mathcal{D}), \overline{\mathcal{U}})$ -reducible (i.e., $((\mathcal{U}_{\text{input}}, \mathcal{U}_{\text{disturbance}}), \mathcal{U}_{\text{kin}})$ -reducible) for every σ . Any $(\mathcal{U}, \mathcal{D}, \mathcal{T})$ -solution must therefore satisfy $V_b \in \text{span}_{\mathbb{R}}\{Y_\alpha\}$. This implies that we can write any solution (which we will denote by Φ_d) as $\Phi_d = \lim_{n \rightarrow \infty} (\amalg_{i, \sigma} \Phi_{\frac{\delta_i}{n} Y_i^\sigma})^n(q_0)$ such that $\sum_i \delta_i = 1$, just as it did in the proof of Lemma 4.1 except that now we are approximating the flow of both the uncertainty and the switching of σ . Piecewise flows can be reduced to a first-order system for each σ by assumption, so we can reduce to a composition of solutions of the form $\lim_{n \rightarrow \infty} (\amalg_{i, \sigma} \Phi_{\frac{\delta_i}{n} X_i^\sigma})^n(q_0)$. Because these are solutions to Eq. (5), and we are taking the Filippov notion of solution, their limit is also a solution [9]. We call this solution Φ_k , and this is a $(\overline{\mathcal{U}}, \mathcal{T})$ -solution to Eq. (5). Hence, if given σ for every $(\mathcal{U}, \mathcal{D}, \mathcal{T})$ -solution we have a $(\overline{\mathcal{U}}, \mathcal{T})$ -solution, we can construct a $(\overline{\mathcal{U}}, \mathcal{T})$ -solution for σ as a measurable function of t . To construct a $(\mathcal{U}, \mathcal{D}, \mathcal{T})$ -solution for a given $(\overline{\mathcal{U}}, \mathcal{T})$ -solution we simply reverse this process and note that any $(\mathcal{U}, \mathcal{T})$ -solution (a dynamic solution without disturbances) is also a $(\mathcal{U}, \mathcal{D}, \mathcal{T})$ -solution. ■

To sum up, if a system of the form in Eq. (3) satisfies the algebraic conditions in Eqs. (6) and (7), the system can be represented as a kinematic system and planning and control can take place in the reduced space without any loss of trajectory information.

4.2 Kinematic Reductions in Closed Loop

Everything discussed so far has implicitly relied on the control being “open-loop.” However, if one is using a discrete time controller (with one’s favorite continuation algorithm, such as zero-order holds) the control is open loop in between controller updates. It was already shown in [18] for two control families \mathcal{U} and $\bar{\mathcal{U}}$ that $(\mathcal{U}, \bar{\mathcal{U}})$ -reductions are not affected by separable discontinuities. By the exact same logic, the systems considered here are reducible in discrete time closed-loop if they satisfy the requirements to be reducible under the tests of Theorem 4.2

Lemma 4.3 *A discrete-time closed loop system (where u^a are functions of q and t) coming from Eq.(3) is $(\mathcal{U}, \mathcal{D}, \bar{\mathcal{U}})$ -reducible to a discrete time version of Eq. (5) if it satisfies the conditions in Theorem 4.2.*

It is also important to note that the systems response to disturbances (in closed-loop) is completely encoded in the reduction as well, precisely because we included the uncertainties in the description of the reduction. Hence, dynamic uncertainties in Eq. (3) become kinematic uncertainties in Eq.(5). This way, closed-loop design in the kinematic description are valid when implemented on the dynamic system, along with a backstepping algorithm to control the velocities of the actuators.

We change the assumption on τ in Eq. (2) slightly by requiring that the reaction force curve must lie in the grayed area in Fig. 5, where $\alpha > 0$. Moreover, assume that that \bar{u} and u are related by $m_i(q)\dot{\bar{u}}_i = \tau u_i$, where $m_i(q) > 0$ is the inertial term for actuator i . That is, the velocity of the contact point is the integral (scaled by the configuration dependent inertia) of the force input, which is common in many applications including those found in Section 2 and 6. Then a choice of backstepping controller

$$u_i = -K(v_i - \bar{u}_i) \quad (9)$$

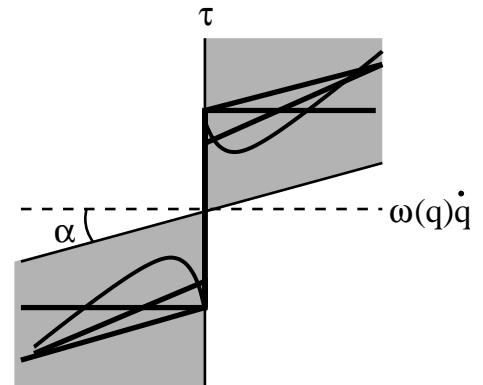


Figure 5: An additional requirement is that the friction curve lie within a sector nonlinearity that allows the use of a proportional controller in implementation.

(where v_i is the desired velocity \bar{u}) provides a stable response because the grayed region is a sector non-linearity [21]. (This result has already been used in the analysis of multi-point contact in [14].) Also, note that the use of a sector nonlinearity also allows us to take into account dynamic shifts in normal force without any extra analysis.

There is no question that better knowledge of the friction law will lead to a model-based controller that performs better. However, we are interested in analyzing cases where the friction model cannot be known. We will see in the example in Section 6.1 that this choice of implementation controller provides acceptable performance (for a variety of friction models) so long as the kinematic controller is stable.

5 Estimation of the Contact State

If one wishes to design a kinematic plan or control of some sort, then online estimation of σ may be necessary. Suppose for any σ we have a stable estimator of $q \in Q$ such that there is a quadratic Lyapunov function V_σ in the error of the state. Then a reasonable estimate of σ (which we will denote $\hat{\sigma}$) could evolve according to

$$\mathbb{E}(y) = \arg \min_{\sigma} \|\tilde{y}_\sigma - \tilde{y}\|$$

where \tilde{y}_σ is the expected output for each σ and \tilde{y} is the measured output. (This assumes that the state evolves differently for every every choice of σ .) However, this estimate may be poor because it may not be stable in the state as σ changes in time. Hence, an adjustment is necessary to estimate both q and σ .

In order to create a stable estimate of σ , we first define some useful notation. First, define

$s(t) = \lim_{\tilde{t} \rightarrow t^-} V_\sigma(\tilde{t}) - \lim_{\tilde{t} \rightarrow t^+} V_\sigma(\tilde{t})$. This is the discrete change in the value of the Lyapunov function for the estimator that occurs when there is a switch in σ . Next define

$$\begin{aligned} \dot{E}(t) &= -k_e \lambda && \text{if } s(t) = 0 \\ E(t) &= \lim_{\tilde{t} \rightarrow t^-} E(\tilde{t}) - s(t) && \text{otherwise} \end{aligned} \tag{10}$$

where k_e is a chosen constant, $0 < k_e < 1$ and $\lambda(t) < 0$ is a bounded conservative estimate of the stability margin for all the estimators that has $\dot{\lambda}$ bounded. For instance, this can sometimes be the minimum

magnitude real part of all of the eigenvalues of all the estimators times the norm of the state if they are based on the linearization. Note that E is initialized to a nonnegative value and then evolves according to Equation 10 as long as s is zero (that is, on intervals with no switches). Whenever $s \neq 0$ (there is a switch), E is re-initialized. Lastly, define $\mathbf{V}_{\sigma(t)}$ to be equal to V_σ on the time intervals between switches. That is, $\mathbf{V}_{\sigma(t)}$ is always equal to the Lyapunov function for a choice of σ on a given time interval. Then we use the following equation to estimate σ .

$$\hat{\sigma}(t) = \begin{cases} \mathbb{E}(\tilde{y}(t)) & \text{if } E > 0 \\ \lim_{\tilde{t} \rightarrow t^-} \mathbb{E}(\tilde{y}(t)) & \text{otherwise} \end{cases} \quad (11)$$

Theorem 5.1 *An estimate of $\hat{\sigma}$ using Eq. (11) converges. That is, $|\mathbf{V}_{\sigma(t)} - \alpha| \rightarrow 0$ for some $\alpha \in \mathbb{R}$ and, in particular, $\dot{\mathbf{V}}_{\sigma(t)} \rightarrow 0$. Moreover, $|\hat{\sigma}(t) - \sigma(t)| = 0$ after a finite amount of time if σ is constant and the state q evolves differently for every choice of σ .*

Proof: For purposes of notational simplicity, we will take \mathbf{V} to denote $\mathbf{V}_{\sigma(t)}$ for the remainder of this proof. Our approach invokes Barbalat's lemma, which states that if $f(t)$ is lower bounded, $\dot{f}(t)$ is negative semi-definite, and $\dot{f}(t)$ is uniformly continuous (or equivalently, $\ddot{f}(t)$ is finite), then $\dot{f}(t)$ approaches zero as t approaches infinity. We will apply Barbalat's lemma to a potential function \mathbf{V}' , thereby showing that $\dot{\mathbf{V}}'$ goes to zero. This, along with the fact that E is monotonically increasing (and therefore, $E > 0$ eventually) between switches implies that $\hat{\sigma}$ can change to $\mathbb{E}(\tilde{y})$ after some finite time.

We will show convergence of the estimator using the function $\mathbf{V}' = \mathbf{V} + E$. Since \mathbf{V} is positive-definite and $E > 0$, it is clear that $\mathbf{V}' \geq 0$. Differentiating, we see that on any interval on which there are no switches we have $\dot{\mathbf{V}}' = \dot{\mathbf{V}} + \dot{E}$. Substituting for \dot{E} we get

$$\dot{\mathbf{V}}' = \dot{\mathbf{V}} - k_e \lambda. \quad (12)$$

To handle switches, note that at a switch in σ we have $\lim_{\tilde{t} \rightarrow t^+} \mathbf{V}(\tilde{t}) = \lim_{\tilde{t} \rightarrow t^-} \mathbf{V}(\tilde{t}) + s(t)$. Thus, at any instant t when a switch occurs (that is, when any $s \neq 0$), we have $\lim_{\tilde{t} \rightarrow t^+} \mathbf{V}'(\tilde{t}) = \lim_{\tilde{t} \rightarrow t^-} \mathbf{V}(\tilde{t}) + s(t) + E(t)$. Substituting for E from Eq. (10), we get $\lim_{\tilde{t} \rightarrow t^+} \mathbf{V}'(\tilde{t}) = \lim_{\tilde{t} \rightarrow t^-} \mathbf{V}(\tilde{t}) + s(t) + \lim_{\tilde{t} \rightarrow t^-} E(\tilde{t}) - s(t)$, which simplifies

in the following way: $\lim_{\tilde{t} \rightarrow t^+} \mathbf{V}'(\tilde{t}) = \lim_{\tilde{t} \rightarrow t^-} \mathbf{V}(t) + \lim_{\tilde{t} \rightarrow t^-} E(\tilde{t}) = \lim_{\tilde{t} \rightarrow t^-} \mathbf{V}'(\tilde{t})$. Thus, the discontinuity in \mathbf{V}' has been removed, as the limits from both sides are the same. Since switches have no effect whatsoever on \mathbf{V}' , Equation 12 holds true at all times.

Since $\dot{\mathbf{V}}$ is negative definite, $0 < k_e < 1$, and $\dot{\mathbf{V}} < k_e \lambda < 0$, it must be the case that $\dot{\mathbf{V}}'$ is negative semi-definite. Moreover, since $\ddot{\mathbf{V}}$ is bounded (because the dynamics are piecewise smooth) and $\dot{\lambda}$ is bounded, we also know $\ddot{\mathbf{V}}'$ is bounded.

We now have sufficient information to satisfy Barbalat's lemma. We know \mathbf{V}' is lower bounded by zero, $\dot{\mathbf{V}}'$ is negative semi-definite, and $\ddot{\mathbf{V}}'$ is bounded, so Barbalat's lemma implies that $\dot{\mathbf{V}}' \rightarrow 0$ as $t \rightarrow \infty$. It follows directly that $\dot{\mathbf{V}}_{\sigma(t)} \rightarrow 0$ as $t \rightarrow \infty$. Moreover, by the monotonically increasing evolution of E between switches in the estimate of σ we are guaranteed to eventually be able to switch to any estimate $\mathbb{E}(\tilde{y})$ of σ .

■

6 Examples

Mechanical systems that experience intermittent contact are common in engineering, and include vehicles such as the Mars Rover [16], distributed manipulation [3,4,14,17], MEMS manipulation [13], and legged locomotion [10]. In these situations, particularly at the micro-scale, the reaction forces due to friction are not well characterized and can involve a host of friction modeling methodologies [20]. Hence, it is desirable to represent these systems in a way that does not involve the frictional reaction forces explicitly.

Note that if the contact state of a $((\mathcal{U}_{\text{input}}, \mathcal{U}_{\text{disturbance}}), \mathcal{U}_{\text{kin}})$ -reducible intermittent contact system is being driven by the frictional interactions (such as the case of MEMS manipulation), *the effects of friction are completely encoded in the σ evolution*. The advantage of this is that it takes a highly nonlinear, nonsmooth phenomenon and encodes its effect as a finite state machine. The examples discussed here illustrate how the prior results can allow one to neglect disturbance forces in mechanical systems. First a slip-steered vehicle is presented and then manipulation using actuator arrays is analyzed.

6.1 Slip-Steered Vehicles

Consider the vehicle in Fig. 2 and diagrammed in Fig.6. The configuration is $q = (x, y, \theta)$ and there are forces u_1, u_2, u_3, u_4 acting on the body at each wheel, where wheel 1 is the front right wheel and then the wheels are numbered counter-clockwise. (One can analyze this system using $q = (x, y, \theta, \phi_1, \phi_2, \phi_3, \phi_4)$ where ϕ_i are the configurations of the wheels with no substantive change in the calculations—it is simplified here for purposes of presentation.) The wheels are located a units to the front and back of the center of mass and b units to the right and left. The inertia tensor for the vehicle is simply $G = m dx \otimes dx + m dy \otimes dy + J d\theta \otimes d\theta$ where m is the mass of

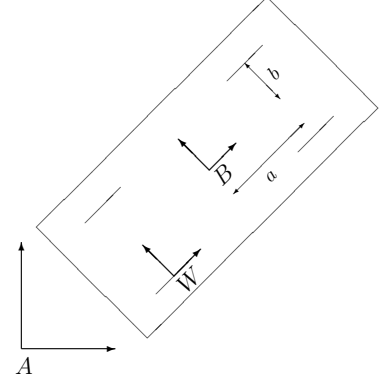


Figure 6: A slip-steered vehicle with frames at each wheel, its center of geometry, and inertial frame.

the vehicle and J its moment of inertia about its center of mass. There are two constraints—that the front wheels cannot slide sideways and that the back wheels cannot slide sideways. Relative to the coordinates $q = [x, y, \theta]$, these can be represented by the covectors

$$\omega_f = [-\sin(\theta), \cos(\theta), a] \quad \omega_b = [-\sin(\theta), \cos(\theta), -a]$$

respectively. The force vector fields Y_i obtained by adjoining the input forces from the wheels into the generalized coordinates are:

$$Y_1 = \begin{bmatrix} \cos(\theta) \\ \sin(\theta) \\ -b \end{bmatrix} \quad Y_2 = \begin{bmatrix} \cos(\theta) \\ \sin(\theta) \\ b \end{bmatrix} \quad Y_3 = \begin{bmatrix} \cos(\theta) \\ \sin(\theta) \\ b \end{bmatrix} \quad Y_4 = \begin{bmatrix} \cos(\theta) \\ \sin(\theta) \\ -b \end{bmatrix},$$

so it is clear that $Y_1 = Y_4$ and $Y_2 = Y_3$.

We now proceed to analyze the slip-steered vehicle. We will make the canonical distinction between $\tau(0)$ (a constraint force) and $\tau(v \neq 0)$ (a slipping force) as before, hence leading to four different possibil-

ities of stick/slip, two for the front wheels and two for the back wheels. We denote the contact state Σ for this system to be the four possible choices of sideways slipping and sticking. That is, $\sigma \in \Sigma$ satisfies $\sigma = 1$ if both constraints are satisfied, $\sigma = 2$ if the front wheels are slipping sideways but the back wheels are not, $\sigma = 3$ if the back wheels are slipping sideways but the front are not, and $\sigma = 4$ if both front and back wheels are sliding sideways. We will see that $\sigma = 1, 2, 3$ are all $((\mathcal{U}_{\text{input}}, \mathcal{U}_{\text{disturbance}}), \mathcal{U}_{\text{kin}})$ -reducible but that $\sigma = 4$ is not $((\mathcal{U}_{\text{input}}, \mathcal{U}_{\text{disturbance}}), \mathcal{U}_{\text{kin}})$ -reducible. Lastly, note that if one of the constraints is broken, and there is a reaction force due to slipping, it will be of the form $V_f = P_\sigma \omega_f^T$ or $V_b = P_\sigma \omega_b^T$, where P_σ is the G -orthogonal projection operator for the contact state σ (see Appendix).

The underlying dynamics evolve on $TSE(2)$ while the frictional forces are $d_{f,b} \in \mathbb{R}$ and $u_i \in \mathbb{R}$ are the set of four input forces (elements of $\mathcal{U}_{\text{input}}$) that can be applied to the body. The kinematics evolve on $SE(2)$, the contact changes due to friction nominally evolve on $\Sigma = \{1, 2, 3, 4\}$ (we will see that 4 cannot be in Σ), and $\tilde{u} \in \mathbb{R}^4$ is a velocity input in \mathcal{U}_{kin} .

For each choice of σ , the equations of motion are of the form

$$\nabla_{\dot{q}}^\sigma \dot{q} = P_\sigma Y_1 u_1 + P_\sigma Y_2 u_2 + P_\sigma Y_3 u_3 + P_\sigma Y_4 u_4 + P_\sigma V_f d_f + P_\sigma V_b d_b.$$

In the case of this vehicle, the affine connections ∇^σ are all trivial, as can be verified by calculation of the constrained affine connection. For each state σ , we compute the equations of motion separately and test whether it is $((\mathcal{U}_{\text{input}}, \mathcal{U}_{\text{disturbance}}), \mathcal{U}_{\text{kin}})$ -reducible. In each case we first compute the projected vector fields and then consider whether the system is reducible. (To simplify notation, let $k_J = J + a^2 m$ in all that follows.)

6.1.1 Analysis of the Slip-Steered Vehicle

No Slipping ($\sigma = 1$): With no wheels slipping sideways we compute the affine connection with both ω_f and ω_b as constraints and the G -orthogonal projection P_1 . The projection P_1 can be computed using the distribution $D = \text{NullSpace}([\omega_b, \omega_f])$ and its complement $D' = \text{NullSpace}(G \cdot D)$ (where G is now the matrix representation of the tensor G). These allow one to compute the projection $P'_1 = AP_1^D A^{-1}$, where

$A = [D|D']$ and $P_1^D = \text{diag}\{1, 1, 0\}$ (this should be thought of as the projection in coordinates aligned with the vector fields that span D and D'). With this, $P_1 = (I_{3 \times 3} - P_1^D)G^{-1}$. (The calculations are nearly identical for $P_2 - P_4$. For more information on these calculations, see [5].) This gives us inputs of the form:

$$P_1 Y_i = \frac{1}{m} \begin{bmatrix} \cos(\theta) \\ \sin(\theta) \\ 0 \end{bmatrix} \forall i$$

There are no V input forces because in this contact state the contacts are maintained. Moreover, $\langle Y_i, Y_j \rangle = 0 \forall i$. Therefore, this system is $((\mathcal{U}_{\text{input}}, \mathcal{U}_{\text{disturbance}}), \mathcal{U}_{\text{kin}})$ -reducible with dynamics $\ddot{q} = P_1 Y_1 u$ and reduction $\dot{q} = P_1 Y_1 \bar{u}$, but is clearly not controllable (since there is only one vector field). Hence, it is desirable to force the vehicle to exit $\sigma = 1$ (e.g., if it needs to turn). However, if the difference between $u_1 + u_4$ and $u_2 + u_3$ is large enough, the stiction constraint force can always be exceeded so that $\sigma \neq 1$.

Front Wheels Slipping ($\sigma = 2$): With the front wheels slipping we compute the affine connection with the constraint ω_b and the reaction force $V_f = P_2 \omega_f^T$. This gives us inputs of the form:

$$P_2 Y_1 = P_2 Y_4 = \frac{1}{mk_J} \begin{bmatrix} k_J \cos(\theta) + abm \sin(\theta) \\ k_J \sin(\theta) - abm \cos(\theta) \\ -bm \end{bmatrix} \quad P_2 Y_2 = P_2 Y_3 = \frac{1}{mk_J} \begin{bmatrix} k_J \cos(\theta) - abm \sin(\theta) \\ abm \cos(\theta) + k_J \sin(\theta) \\ bm \end{bmatrix}$$

and $\langle P_2 Y_1, P_2 Y_1 \rangle, \langle P_2 Y_2, P_2 Y_2 \rangle, \langle P_2 Y_1, P_2 Y_2 \rangle \in \text{span}_{\mathbb{R}}\{P_2 Y_1, P_2 Y_2\}$, so it satisfies the first requirement in Eq. (6) to be $((\mathcal{U}_{\text{input}}, \mathcal{U}_{\text{disturbance}}), \mathcal{U}_{\text{kin}})$ -reducible. Computing V_f (the reaction force due to the front wheels slipping sideways), we see that

$$V_f = P_2 \omega_f^T = \begin{bmatrix} -2a^2 \sin(\theta) \\ 2a^2 \cos(\theta) \\ 2a \end{bmatrix} \in \text{span}_{\mathbb{R}}\{P_2 Y_1, P_2 Y_2\}$$

so this system is $((\mathcal{U}_{\text{input}}, \mathcal{U}_{\text{disturbance}}), \mathcal{U}_{\text{kin}})$ -reducible with dynamics $\ddot{q} = P_2 Y_1 u_1 + P_2 Y_2 u_2$ and reduction

$$\dot{q} = P_2 Y_1 \bar{u}_1 + P_2 Y_2 \bar{u}_2.$$

Back Wheels Slipping ($\sigma = 3$): The back wheels slipping sideways while the front wheels do not slip is essentially the same as $\sigma = 2$. We get

$$P_3 Y_1 = P_3 Y_4 = \frac{1}{mk_J} \begin{bmatrix} k_J \cos(\theta) - abm \sin(\theta) \\ abm \cos(\theta) + k_J \sin(\theta) \\ -bm \end{bmatrix} \quad P_3 Y_2 = P_3 Y_3 = \frac{1}{mk_J} \begin{bmatrix} k_J \cos(\theta) + abm \sin(\theta) \\ k_J \sin(\theta) - abm \cos(\theta) \\ bm \end{bmatrix}$$

and computing V_b we get

$$V_b = P_2 \omega_b^T = \begin{bmatrix} -2a^2 \sin(\theta) \\ 2a^2 \cos(\theta) \\ -2a \end{bmatrix} \in \text{span}_{\mathbb{R}}\{P_3 Y_1, P_3 Y_2\}$$

leading to the system being $((\mathcal{U}_{\text{input}}, \mathcal{U}_{\text{disturbance}}), \mathcal{U}_{\text{kin}})$ -reducible with reduction $\dot{q} = P_3 Y_1 \bar{u}_1 + P_3 Y_2 \bar{u}_2$.

All Wheels Slipping ($\sigma = 4$): The case where both axles slip sideways is the one of most interest, as it will turn out to not be $((\mathcal{U}_{\text{input}}, \mathcal{U}_{\text{disturbance}}), \mathcal{U}_{\text{kin}})$ -reducible. Since there are no constraints, P_4 is simply G^{-1} . This gives us

$$P_4 Y_1 = P_4 Y_4 = \frac{1}{mJ} \begin{bmatrix} J \cos(\theta) \\ J \sin(\theta) \\ -bm \end{bmatrix} \quad P_4 Y_2 = P_4 Y_3 = \frac{1}{mJ} \begin{bmatrix} J \cos(\theta) \\ J \sin(\theta) \\ bm \end{bmatrix}$$

and again $\langle P_4 Y_1, P_4 Y_1 \rangle, \langle P_4 Y_2, P_4 Y_2 \rangle, \langle P_4 Y_1, P_4 Y_2 \rangle \in \text{span}_{\mathbb{R}}\{P_4 Y_1, P_4 Y_2\}$, so it satisfies the requirement in Eq. (6) to be $((\mathcal{U}_{\text{input}}, \mathcal{U}_{\text{disturbance}}), \mathcal{U}_{\text{kin}})$ -reducible. Therefore, if there were no other forces acting on the system, this would be a reducible system. However, computing V_f and V_b yields

$$V_f = P_4 \omega_f^T = \frac{1}{mJ} \begin{bmatrix} -J \sin(\theta) \\ J \cos(\theta) \\ am \end{bmatrix} \notin \text{span}_{\mathbb{R}}\{P_4 Y_1, P_4 Y_2\}$$

and

$$V_b = P_4 \omega_b^T = \frac{1}{mJ} \begin{bmatrix} -J \sin(\theta) \\ J \cos(\theta) \\ -am \end{bmatrix} \notin \text{span}_{\mathbb{R}}\{P_4 Y_1, P_4 Y_2\}$$

so this system is *not* $((\mathcal{U}_{\text{input}}, \mathcal{U}_{\text{disturbance}}), \mathcal{U}_{\text{kin}})$ -reducible. This means that when $\sigma = 4$, a kinematic description of the system cannot be used for planning or feedback control.

6.1.2 Design implications and Simulations

Now let us use the kinematic description to create a motion planner that is not sensitive to the particulars of friction in a planar setting. Since $\sigma = 1, 2, 3$ are kinematic and $\sigma = 4$ is not, $\sigma = 4$ should be considered unsafe and avoided. Of course the system is not controllable when $\sigma = 1$, so we should only allow the system to have $\sigma = 1$ when the vehicle is already oriented properly and does not need to turn.

The approach taken here is to simply initially ignore the fact that σ changes and pretend that the system is differentially flat with output x and y . We construct a path $(x_d(t), y_d(t))$ and follow it using the control law

$$\bar{u}_1 = \bar{u}_4 = K_\theta(\theta_d - \theta) + K_s r \quad (13)$$

$$\bar{u}_2 = \bar{u}_3 = -K_\theta(\theta_d - \theta) + K_s r \quad (14)$$

where θ_d is the desired orientation, r is the x component of the body representation of the desired trajectory, and K_θ and K_s are control gains to be chosen. The controls \bar{u}_i are implemented dynamically using Eq. (9) and the estimation of σ is achieved assuming full-state feedback so that Eq.(11) can be used with *any* nonzero, negative value of the estimated stability margin λ . Note that for K_θ and $\theta_d - \theta$ large enough, any finite stiction μ_S coefficient will be exceeded and the vehicle will leave $\sigma = 1$. Moreover, if the vehicle is in a state with $\sigma = 4$, reducing u_i (by reducing gains or directly saturating \bar{u}_i in Eq. (9)) will always move the system back into $\sigma = 1, 2, 3$).

Figure 7 shows simulations of this scenario with a full dynamic model (including the configuration of

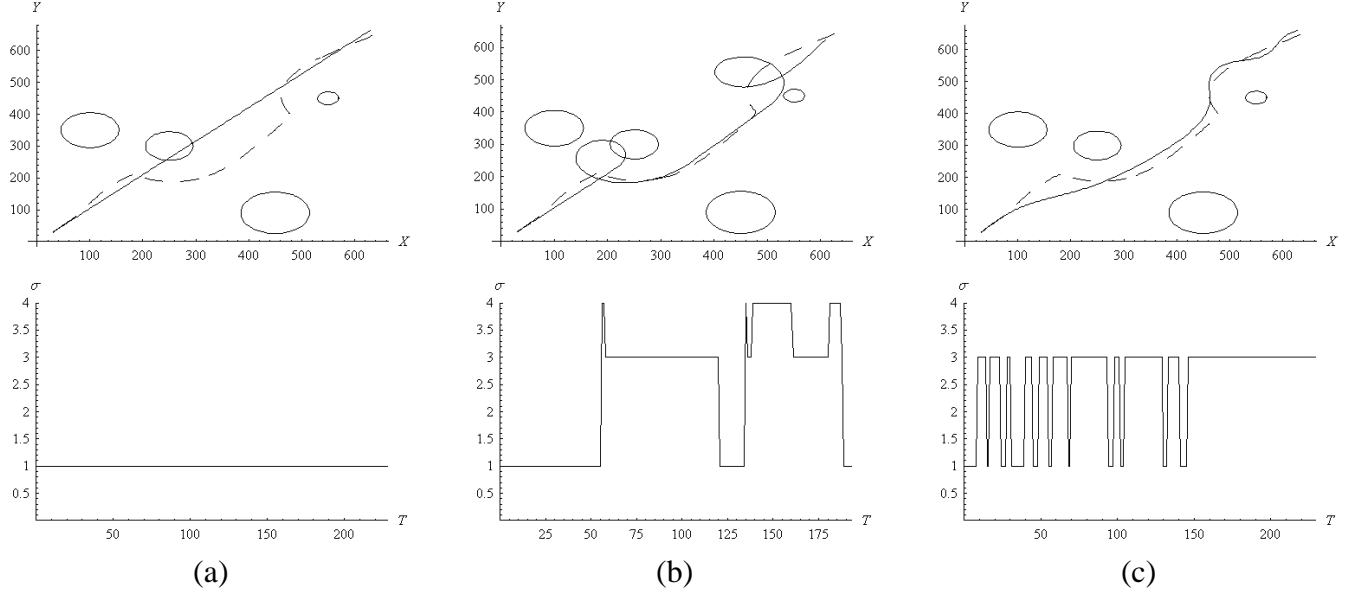


Figure 7: Simulations of the slip-steered vehicle. The graphs on top show the XY trajectory of the vehicle and elliptical obstacles it should avoid while the plots on bottom show how σ , the contact state, changes over time. These simulations show poor performance in (a) due to staying in $\sigma = 1$ (an uncontrollable kinematic state) and in (b) due to transitioning into a dynamic mode where the kinematic plan is not valid. Saturating the inputs so that the system stays in the kinematic modes leads to acceptable performance in (c).

the wheels, so that $q = (x, y, \theta, \phi_1, \phi_2, \phi_3, \phi_4)$ where ϕ_i are the configurations of the wheels). Parameters came from the vehicle in Fig.2, and were geometry ($a = 15cm$, $b = 10cm$), the mass of the body of the vehicle ($m_b = 60Kg$), the mass of the wheels ($m_w = 10Kg$), radius of wheels ($r_w = 8cm$), and Coulomb viscous friction ($\mu_S = .6N$, $\mu_K = 1N/(m/s)$). The switching in σ (i.e., the automaton over $\Sigma = \{1, 2, 3, 4\}$) is based on calculating the Lagrange multipliers for the constrained dynamics and evaluating whether the multipliers exceed the Coulomb friction coefficient μ_S . All bodies were considered homogeneous for purpose of calculating their inertia tensors. Figure 7 shows two graphs for three different situations. The top graph shows the x and y trajectory of the vehicle, with the dotted line being the desired path and the black line being the actual trajectory. The ellipses are obstacles, and the obstacle-free desired path (x_d, y_d) was computed using a potential-based planner [11]. The bottom graph shows σ as a function of time.

Figure 7(a) shows $K_\theta = 2000$ and $K_s = 0.005$ (these differences in magnitude are due to choice of units). Because K_θ is too small, the vehicle never leaves $\sigma = 1$ and crashes into an obstacle. Figure 7(b)

shows a more aggressive controller of $K_\theta = 3000$ and $K_s = 0.01$, and we see the vehicle gets off course because of sideways slip and again runs into an obstacle. It generally has bad dynamic behavior (later it runs in a loop sliding sideways), indicating that a controller would need to take dynamic effects into account. Figure 7(c) shows an even more aggressive controller of $K_\theta = 8000$ and $K_s = 0.013$ where now the velocity commands are saturated if they are going to push the system into $\sigma = 4$. Hence, not only do we see successful avoidance of obstacles, but we additionally see that the system never enters $\sigma = 4$. Notice that this implies that “fish-tailing” (where the back wheels slide sideways) is fine from a kinematic perspective whereas all wheels sliding sideways is not acceptable in terms of kinematic analysis.

Note that we cannot ask for anything more than bounding the error because there is always a sufficiently low orientation error that we enter $\sigma = 1$ (where we cannot stabilize to the trajectory), hence leading to substantial error even in Fig. 7(c) between $100m$ and $200m$ in x and y and between times $30s$ and $50s$ when the vehicle is staying in $\sigma = 1$. Nevertheless, even this naive controller with only minimal representation of the underlying frictional dynamics functions well enough to ensure adequate path following.

The key point is that planning for this vehicle can be done on a purely kinematic basis so long as $\sigma = 1, 2, 3$. This condition requires a slight modification to ensure that $\sigma \neq 4$, but does not require any detailed information about the mechanical contact.

The last thing to note is that the bottom plots of σ versus time give a good indication that fully modeling $\tau \in \mathcal{L}$ is not necessary for purposes of estimating σ ; σ evolves rather slowly. We will discuss this more in detail in the next section on actuator arrays.

6.2 Actuator Arrays

Consider Fig. 8. In this schematic we see a chip on an insulating layer that is actuated by nine SDAs (discussed in Section 2). Each SDA is capable of moving in the direction of its long axis and is in principle constrained to not move sideways. If it does move sideways, a reaction force occurs due to the sliding. Such a chip can be viewed as a micro-scale vehicle capable of “driving” on the insulating layer [13], or, if flipped over, could function as a manipulation surface. Now we ask whether such a chip can be represented

as a kinematic system.

Assume that the chip has mass m and rotational inertia J , so that when we write the coordinates of its body frame relative to the world as $q = (x, y, \theta)$, $G = m dx \otimes dx + m dy \otimes dy + J d\theta \otimes d\theta$. The dynamics evolve on $TSE(2)$ and the friction reaction forces are in \mathcal{L}^r , where r is the number of actuators. The kinematic equations evolve on $SE(2)$ and Σ is a finite set that describes the total number of contact states for the system. For simplicity, assume that the SDA actuators are themselves of negligible mass and that they form a point contact with the insulating layer. Then, the equations of motion can be written as $\nabla_{c'(t)} c'(t) = u^a Y_a + d^b V_b$. In this equation the u^a correspond to each force being produced by the SDAs and the Y_a transform these forces into the body frame while respecting any constraints imposed upon the system. Such constraints arise from no-slip contact between the insulating layer and the actuators. The d^b represent reaction

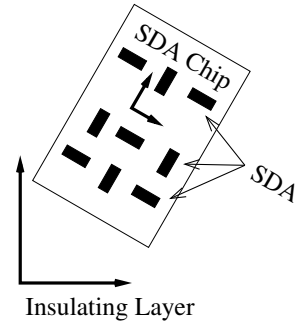


Figure 8: Array of scratch drive actuators

forces due to slipping along the insulating layer when such a constraint is violated. We now analyze whether a planar array of alternately orthogonal actuators (such as those seen in Fig. 8) is kinematic.

Proposition 6.1 *An object manipulated by a planar array of alternatively orthogonal actuators has dynamics that are both $(\mathcal{U}_{input}, \mathcal{U}_{disturbance})$ -reducible and $((\mathcal{U}_{input}, \mathcal{U}_{disturbance}), \mathcal{U}_{kin})$ -reducible.*

Proof: Note that we cannot explicitly compute all possible equations of motion for an infinite array of actuators. Instead, we implicitly show that the conditions for reducibility are met. First, it is clear that the system is $(\mathcal{U}_{input}, \mathcal{U}_{disturbance})$ -reducible. This follows from the fact that in the body frame any reaction force due to friction is a vector in $\mathbb{R}^3 \cong se^*(2)$ (the dual to the Lie algebra of $SE(2)$), and the forces coming from the actuators span \mathbb{R}^3 . This fact is not surprising because the system is massively overactuated, but it is unfortunately also not terribly helpful due to the fact that we cannot reliably compute the reaction forces.

We are now left with the question of whether the pictured SDA chip is $((\mathcal{U}_{input}, \mathcal{U}_{disturbance}), \mathcal{U}_{kin})$ -reducible. Note that if we represent the chip as a rigid body with configuration in $SE(2)$, any force vector

\vec{f} at an actuator A_i can be represented in the inertial frame by a wrench in $se^*(2)$, namely $Ad_{g_{WB}g_{BA_i}}^T \vec{f}$. In this formula g_{WB} is the rigid body transformation from the world frame to the body frame, g_{BA_i} is the rigid body transformation from the body frame to the actuator frame, and $Ad_{g_{XY}}$ is the adjoint transformation mapping velocities in the Y frame to velocities in the X frame. (For an elementary presentation of these computations, see [19].) Hence, if we assume that forces (from constraints or from actuation) occur at the site of actuators A_i , we can compute their forces in the common inertial frame, and thus compute $u^a Y_a + d^b V_b$. Say that we choose three actuators, A_1 , A_2 , and A_3 , each with coordinates in the body frame (a_i, b_i, ψ_i) , where ψ_i are multiples of $\frac{\pi}{2}$ (since the actuators are all orthogonal). Then, if we assume that the location of the body in the world frame is (x, y, θ) , the representation of each of the forces in the world frame can be written as $Ad_{g_{WB}g_{BA_i}}^T \vec{f}_i = [\cos(\theta + \psi_i), -\sin(\theta + \psi_i), y + b \cos(\theta) + a \sin(\theta)]^T$. If we take the determinant of the matrix $[Ad_{g_{WB}g_{BA_1}}^T \vec{f}_1, Ad_{g_{WB}g_{BA_2}}^T \vec{f}_2, Ad_{g_{WB}g_{BA_3}}^T \vec{f}_3]$ we find that it is nonzero as long as $\psi_1 \neq \psi_2$. Hence, alternately orthogonal is not really a necessary condition—instead alternately skew is necessary.

First, what does this mean if there are no constraints (i.e., no slipping orthogonal to the actuators). Then for the proper choice of actuators, $\mathbb{R}^3 = T_{(x,y,\theta)}SE(2)$ is spanned by the force vector fields $u^a Y_a$, so the system without disturbance forces is $(\mathcal{U}_{\text{dyn}}, \mathcal{U}_{\text{kin}})$ -reducible by Lemma A.2 (in Appendix) which implies that with forces it is $(\mathcal{U}_{\text{input}}, \mathcal{U}_{\text{disturbance}}, \mathcal{U}_{\text{kin}})$ -reducible by Lemma 4.3. If there is only one constraint, then for the proper choice of input forces u^a that constraint combined with Y_a span \mathbb{R}^3 , implying by similar logic that the dynamic system with disturbances is $(\mathcal{U}_{\text{input}}, \mathcal{U}_{\text{disturbance}}, \mathcal{U}_{\text{kin}})$ -reducible. The argument for two constraints is identical. For three independent constraints, the chip is completely constrained not to move. ■

Hence, an array of actuators manipulating an object is always $(\mathcal{U}_{\text{input}}, \mathcal{U}_{\text{disturbance}}, \mathcal{U}_{\text{kin}})$ -reducible to a kinematic system of the form in Eq. (4). Moreover, as the contact states change, the kinematic system will change. This means that the effects of friction on the dynamics of the chip are now completely encoded in the switching of σ from one set of *kinematic* equations to another over time. This situation has well-defined control strategies, as discussed next.

Table 1: Orthogonal Actuator arrays (like those seen in Fig. 8 and Fig. 8) have all kinematic states, many of which are redundant. This figure shows the four distinct equations of motion that can occur. Note that so long as $\bar{u}_{(1,1)}$ ($= \bar{u}_{(-1,-1)}$) and $\bar{u}_{(-1,1)}$ ($= \bar{u}_{(1,-1)}$) are nonzero, the four states can be distinguished from state output. In fact, just observation of θ is sufficient for distinguishing the states. Moreover, this system can be stabilized to the origin using the control law shown and an estimate of σ [15].

σ	Equations of Motion					Control Law
$\sigma = 1$	$\dot{q} =$	$\begin{bmatrix} -1 \\ -1 \\ 0 \end{bmatrix}$	$\bar{u}_{(1,1)} +$	$\begin{bmatrix} 1 \\ -1 \\ 1 \end{bmatrix}$	$\bar{u}_{(-1,1)}$	$\bar{u}_{(1,1)} = \frac{-k\theta(\theta+x-y)+k(\theta^2+x^2+y^2)}{x+y}$ $\bar{u}_{(-1,1)} = -k\theta$
$\sigma = 2$	$\dot{q} =$	$\begin{bmatrix} -1 \\ -1 \\ -1 \end{bmatrix}$	$\bar{u}_{(1,1)} +$	$\begin{bmatrix} 1 \\ -1 \\ 0 \end{bmatrix}$	$\bar{u}_{(-1,1)}$	$\bar{u}_{(1,1)} = k\theta$ $\bar{u}_{(-1,1)} = \frac{k\theta(\theta+x+y)-k(\theta^2+x^2+y^2)}{x-y}$
$\sigma = 3$	$\dot{q} =$	$\begin{bmatrix} -1 \\ -1 \\ 0 \end{bmatrix}$	$\bar{u}_{(1,1)} +$	$\begin{bmatrix} 1 \\ -1 \\ -1 \end{bmatrix}$	$\bar{u}_{(-1,1)}$	$\bar{u}_{(1,1)} = \frac{k\theta(\theta-x+y)+k(\theta^2+x^2+y^2)}{x+y}$ $\bar{u}_{(-1,1)} = k\theta$
$\sigma = 4$	$\dot{q} =$	$\begin{bmatrix} -1 \\ -1 \\ 1 \end{bmatrix}$	$\bar{u}_{(1,1)} +$	$\begin{bmatrix} 1 \\ -1 \\ 0 \end{bmatrix}$	$\bar{u}_{(-1,1)}$	$\bar{u}_{(1,1)} = -k\theta$ $\bar{u}_{(-1,1)} = \frac{-k\theta(-\theta+x+y)-k(\theta^2+x^2+y^2)}{x-y}$

6.2.1 Stabilization of Manipulation Using Arrays of Actuators

Consider a desired equilibrium point on an alternately orthogonal array. It has contact actuators located at $(2i + 1, 2j + 1)$ with $i, j \in \mathbb{N}$. Their orientations relative to the world frame are alternately $\frac{\pi}{4}$ and $-\frac{\pi}{4}$, and the applied force is always in the direction of the x -axis of the local actuator frame. We will denote the velocities of these actuators by $\bar{u}_{(2i+1,2j+1)}$ and the applied force by $u_{(2i+1,2j+1)}$. The system is $((\mathcal{U}_{\text{input}}, \mathcal{U}_{\text{disturbance}}), \mathcal{U}_{\text{kin}})$ -reducible by Prop. 6.1, so long as the contact interfaces are *dissipative* when slipping is occurring (i.e., the reaction force is nonzero and in the opposite direction of the slipping). The dynamics are of the form

$$M\ddot{q} = \sum_{(2i+1,2j+1)} Ad_{g_{(2i+1,2j+1)}}^T \begin{bmatrix} 1 \\ 0 \\ 0 \end{bmatrix} u_{(2i+1,2j+1)} + Ad_{g_{(2i+1,2j+1)}}^T \begin{bmatrix} 0 \\ 1 \\ 0 \end{bmatrix} d_{(2i+1,2j+1)} + \Lambda^T \omega(q)^T \quad (15)$$

where $q = (x, y, \theta)$, $\omega(q)$ is the set of constraint covectors, g_i is the rigid body mapping from the world frame to the actuator i frame, Λ is the vector of Lagrange multipliers, and $M = \text{diag}\{m, m, J\}$. The

Lagrange multipliers are solved for using the constraint equation $\frac{d}{dt}(\omega(q)\dot{q}) = 0$. Additionally, all the nontrivial, non-overconstrained kinematics when the center of mass is near $(x, y) = (0, 0)$ are of one of the four forms in Table 6.2.1 [15, 17].

For each of the four models in Table 6.2.1 a control law is calculated from the Lyapunov function $k(x^2 + y^2 + \theta^2)$ (where k is some constant to be chosen during implementation) by solving $\dot{V} = -V$ for $\bar{u}_{(2i+1, 2j+1)}$ subject to the constraint that actuators with the same orientation have the same velocity command \bar{u} . Hence, there are two unique inputs $\bar{u}_{(1,1)}$ and $\bar{u}_{(-1,1)}$ in the kinematic description, and including more does not produce additional trajectories [15, 17]. Moreover, by virtue of the design methodology, there is a common Lyapunov function. This was shown to provide global stabilization to $(0, 0, 0)$ for the kinematic system in [15, 17].

Figure 9 shows three simulations of an actuator array near a desired equilibrium. For each simulation, going from left to right, the XY location of a manipulated object is shown, the orientation θ , the evolution of σ , and the response of the actuator at $(1, 1)$ in the dynamic simulation as it tracks $\bar{u}_{(1,1)}$. The four actuators near the equilibrium dominate the motion, and the rest are kinematically constrained to match the speeds of $u_{(1,1)}$ and $u_{(-1,1)}$. We use Eq. (9) to implement the commands $\bar{u}_{(2i+1, 2j+1)}$ with a control gain of $K = 10$ for three different friction laws—Coulomb friction, viscous friction, and stiction, as in Section 3.1. Again the contact state is estimated using Eq.(11) with full-state feedback. All the responses have an initial condition of $(x_0, y_0, \theta_0) = (0.5, 2, \frac{\pi}{2})$ and the goal is to stabilize to the origin $(0, 0, 0)$. All responses are qualitatively similar despite the differences in friction law in the actual implementation.

The key is that despite changes in the characteristics of friction, the controller computed based on the kinematic equations of motion (which only needs to estimate σ) performs well (and similarly to the macro-scale experimental work in [17]). This is because all possible σ yield kinematic equations of motion that can be stably implemented using Eq. (9).

Lastly, note that σ does not change very quickly in this setting, just as it did not change very quickly in Fig. 7 in Section 6.1. Moreover, looking at the kinematic equations of motion, we see that σ can be estimated based on θ measurements alone (so long as $\bar{u}_1 \neq \bar{u}_2$ and $\bar{u}_1, \bar{u}_2 \neq 0$). In this case sensing θ at 10 Hz would be more than sufficient for purposes of capturing the σ changes. In comparison to directly

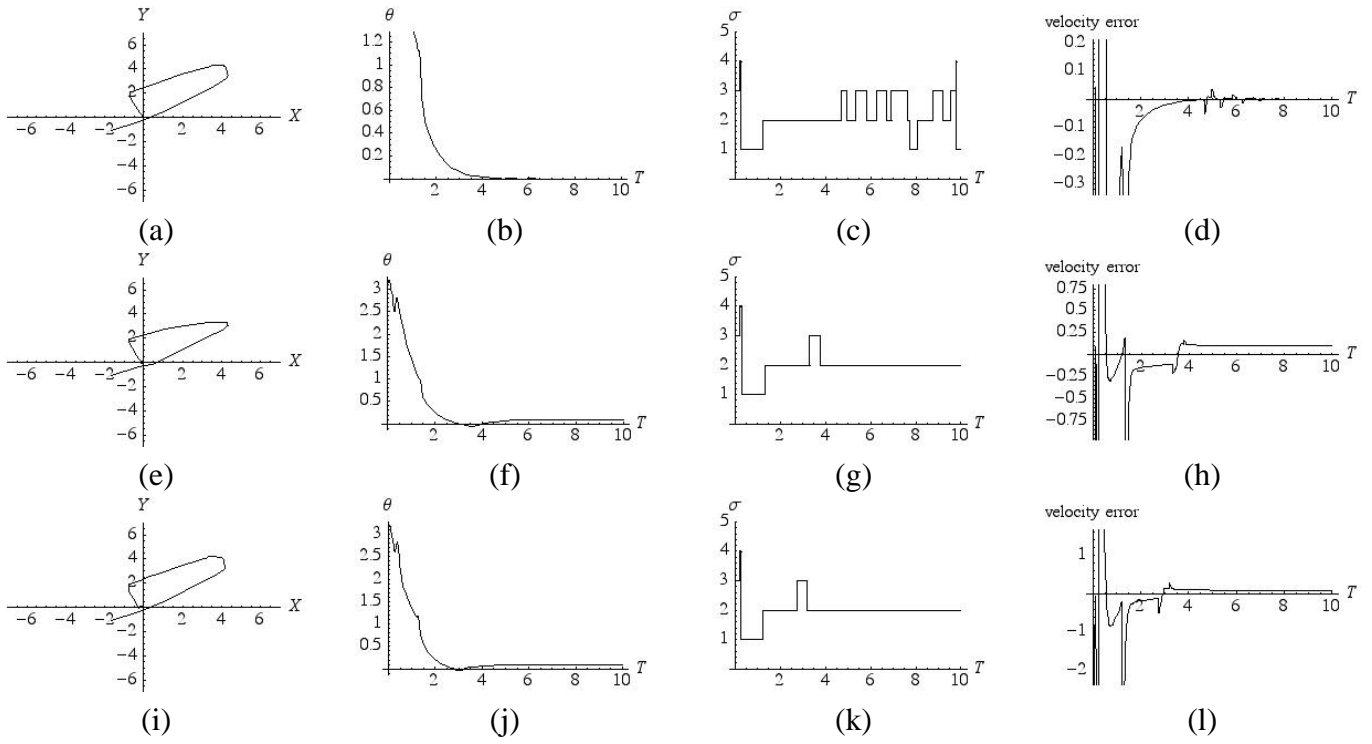


Figure 9: Three simulations with different choices of friction model. From left to right, the plots are the XY trajectory of an object supported by an actuator array, the orientation θ as a function of time, the kinematic state σ as a function of time, and lastly the response of the actuator at $(1, 1)$ as it tracks the desired velocity $\bar{u}_{(1,1)}$. The simulations are for viscous friction (a-d), Coulomb friction (e-h), and stiction friction (i-l). Parameters used were $m = 1$, $J = 5$, $\mu_S = 1.1$, $\mu_K = 1$, and $K = 10$ in Eq. (9).

identifying $\tau \in \mathcal{L}$, which often requires sampling rates at 1 KHz or more, this is clearly superior from a sensing perspective.

7 Conclusions

This paper considers the use of a canonical distinction between slipping frictional forces and nonslipping frictional forces for purposes of motion planning and control for mechanical contact systems. Geometric kinematic reductions play a central role in why this choice is effective in generating useful descriptions of a system, even when a system experiences stick/slip phenomena (which are typically thought of as being dynamic). Both planning and stabilization can be computed in the kinematic setting, and then implemented in the underlying dynamic space through the use of a stable plan, typically just a backstepping controller in the context of the work presented here. These techniques are illustrated on two example simulations—a slip-steered vehicle and an actuator array. Lastly, the kinematic equations have more limited sensing requirements, both in terms of spatial resolution and temporal resolution. Ongoing work targets demonstrating these results in hardware experiments.

Acknowledgements

The author gratefully acknowledges the support for this work provided by the NSF under CAREER award CMS-0546430. Moreover, the author would like to thank Tim Caldwell for creating the simulation package for the slip-steering vehicle.

References

- [1] T. Akiyama and K. Shonu. Controlled stepwise motion in polysilicon micro-structures. *Journal of Microelectromechanical Systems*, 2(3):106–110, 1993.
- [2] A. Bicchi and V. Kumar. Robotic grasping and contact: a review. In *IEEE Int. Conf. on Robotics and Automation (ICRA)*, pages 348–353, 2000.
- [3] K. Böhringer, B. Donald, and N. MacDonald. Upper and lower bounds for programmable vector fields with applications to mems and vibratory plate parts feeders. In *Algorithms for Robotic Motion and Manipulation*, pages 255–276. A.K. Peters, Ltd., 1997.
- [4] K. F. Böhringer, B. R. Donald, L. E. Kavraki, and F. Lamiroux. A distributed, universal device for planar parts feeding: unique part orientation in programmable force fields. In *Distributed Manipulation*, pages 1–28. Kluwer, 2000.
- [5] F. Bullo and A. Lewis. *Geometric Control of Mechanical Systems*. Number 49 in Texts in Applied Mathematics. Springer-Verlag, 2004.
- [6] F. Bullo and A. Lewis. Low-order controllability and kinematic reductions for affine connection control systems. *SIAM Journal on Control and Optimization*, 44(3):885–908, 2005.
- [7] F. Bullo and K. Lynch. Kinematic controllability and decoupled trajectory planning for underactuated mechanical systems. In *IEEE Int. Conf. on Robotics and Automation (ICRA)*, pages 3300–3307, 2001.
- [8] F. Bullo and K. M. Lynch. Kinematic controllability for decoupled trajectory planning in underactuated mechanical systems. *IEEE Transactions on Robotics and Automation*, 17(4):402–412, August 2001.
- [9] A. Filippov. *Differential Equations with Discontinuous Right-Hand Sides*. Kluwer, 1988.
- [10] B. Goodwine and J. Burdick. Controllability of kinematic control systems on stratified configuration spaces. *IEEE Trans. on Automatic Control*, 46(3):358–368, 2000.

- [11] S. LaValle. *Planning Algorithms*. Cambridge Press, 2006.
- [12] A. Lewis. When is a mechanical control system kinematic? In *Proc. 38th IEEE Conf. on Decision and Control*, pages 1162–1167, Dec. 1999.
- [13] R. Linderman and V. Bright. Nanometer precision positioning robots utilizing optimized scratch drive actuators. *Sensors and Actuators A*, 91:292–300, 2001.
- [14] J. Luntz, W. Messner, and H. Choset. Distributed manipulation using discrete actuator arrays. *Int. J. Robotics Research*, 20(7):553–583, July 2001.
- [15] T. D. Murphey. On multiple model control for multiple contact systems. *Automatica*, Accepted for Publication.
- [16] T. D. Murphey and J. W. Burdick. A controllability test and motion planning primitives for overconstrained vehicles. In *Proc. IEEE Int. Conf. on Robotics and Automation*, pages 2716–2722, Seoul, Korea, 2001.
- [17] T. D. Murphey and J. W. Burdick. Feedback control for distributed manipulation with changing contacts. *International Journal of Robotics Research*, 23(7/8):763–782, July 2004.
- [18] T. D. Murphey and J. W. Burdick. The power dissipation method and kinematic reducibility of multiple model robotic systems. *IEEE Transactions on Robotics*, 22(4):694–710, August 2006.
- [19] R. Murray, Z. Li, and S. Sastry. *A Mathematical Introduction to Robotic Manipulation*. CRC Press, 1994.
- [20] H. Olsson, K. Astrom, C. C. de Wit, M. Gafvert, and P. Lischinsky. Friction models and friction compensation. *European Journal of Control*, 4(3):176–195, 1998.
- [21] M. Vidyasagar. *Nonlinear Systems Analysis*. Prentice Hall, 1978.

A Background: Kinematic Reduction

In discussing kinematic reductions, we follow [5, 6]. A *simple mechanical control system* consists of a manifold Q of dimension n , a Riemannian metric G that defines the kinetic energy, a set of constraints represented as a constraint distribution D , and a set of external forces. Associated with a Riemannian metric G are what are called *Christoffel symbols*.

Definition A.1 *The Christoffel symbols associated with the metric G are*

$${}^G\Gamma_{jk}^i = \frac{1}{2}G^{il} \left(\frac{\partial G_{jl}}{\partial q^k} + \frac{\partial G_{kl}}{\partial q^j} - \frac{\partial G_{jk}}{\partial q^l} \right) \quad (16)$$

where summation over repeated indices is implied used unless otherwise stated, and upper indices indicate the inverse.

Also associated with the Riemannian metric is the *affine connection*, which assigns to a pair of vector fields X and Y another vector field $\nabla_X Y$. This is referred to as the *covariant derivative* of Y with respect to X .

Definition A.2 *In coordinates, the covariant derivative of Y with respect to X is*

$${}^G\nabla_X Y = \left(\frac{\partial Y^i}{\partial q^j} X^j + \Gamma_{jk}^i X^j Y^k \right) \frac{\partial}{\partial q^i} \quad (17)$$

With this, the Euler-Lagrange equations can be written as

$${}^G\nabla_{c'(t)} c'(t) = u^a(t) Y_a(c(t)) \quad (18)$$

where $t \mapsto c(t)$ is a path on Q and $c'(t) = \frac{d}{dt}c(t)$ [5, 6]. In this equation ${}^G\nabla$ is the constrained affine connection associated with the Riemannian metric (kinetic energy) G and Y_a are force vector fields associated with forces u^a . In coordinates this is written as:

$$\ddot{q}^i + {}^G\Gamma_{jk}^i \dot{q}^j \dot{q}^k = u^\alpha Y_\alpha^i. \quad (19)$$

Constrained systems, those control systems whose trajectories must lie in some distribution D , can also be described by Eq. (18). However, the affine connection must be modified in order to incorporate the constraints. Let D be a distribution on Q and let D^\perp denote the G -orthogonal complement of D . Moreover, let $P : TQ \rightarrow TQ$ be a G -orthogonal projection operator onto D and let $P' : TQ \rightarrow TQ$ be a G -orthogonal projection onto D^\perp . Lastly, let $A(q)$ be any invertible $(1, 1)$ tensor field on Q and let $B(q)$ be its inverse. Then, the Euler-Lagrange equations can be written as Eq. (19) where the Christoffel symbols are:

$${}^A\Gamma_{jk}^i = {}^G\Gamma_{jk}^i + B_l^i \frac{\partial (AP')_j^l}{\partial q^k} + B_l^i {}^G\Gamma_{km}^l (AP')_j^m - B_l^i {}^G\Gamma_{kj}^m (AP')_m^l$$

where, again, $A(q)$ is *any* invertible $(1, 1)$ tensor on Q . In order to add forces, we must ensure the forces comply with the constraints. Hence, the final equations of motion are:

$${}^G\nabla_{c'(t)} c'(t) = u^\alpha(t) P_j Y_\alpha^j(c(t)) \quad (20)$$

or in coordinates:

$$\ddot{q}^i + {}^A\Gamma_{jk}^i \dot{q}^j \dot{q}^k = u^\alpha P_j Y_\alpha^i. \quad (21)$$

Therefore, simple mechanical control systems *all* can be represented using an affine connection. For more details and examples worked out in detail, refer to Bullo and Lewis [5].

We know that Eq. (18) is a second order differential equation evolving on the manifold Q . On the other hand, given input velocities \bar{u}^α , *kinematic* equations can be written in the form:

$$\dot{q}(t) = \bar{u}^\alpha(t) X_\alpha(q(t)) \quad (22)$$

Our goal in this section is to formally reduce Eq. (18) to Eq. (22). If $\{X_i\}$ are kinematic vector fields and $\{Y_j\}$ are dynamic vector fields, we let the *distributions* D_{kin} and D_{dyn} be defined by $D_{kin} = \text{span}_{\mathbb{R}}\{X_i\}$ and $D_{dyn} = \text{span}_{\mathbb{R}}\{Y_j\}$. A solution to a control system is defined as follows.

Definition A.3 Let Σ_s be a smooth control system $\dot{q} = f(q, u)$ on a smooth manifold M and let $u \in U \subseteq \mathbb{R}^m$. A (U, T) -solution to Σ_s is a pair (c, u) , where $u : [0, T] \rightarrow U$ and $c : [0, T] \rightarrow M$ satisfy

$$c'(t) = f(c(t), u(t)).$$

Note that Def. A.3 only makes sense for first order equations evolving on M and Eq. (18) is a second order differential equation evolving on Q . Hence, we must rewrite Eq. (18) as a first order equation evolving on TQ . To do this, we must use the *vertical lift*, defined by

$$\text{verlift}(X)(v_q) = \left. \frac{d}{dt} \right|_{t=0} v_q + tX(q),$$

and the *geodesic spray*, defined in coordinates by

$$Z = v^i \frac{\partial}{\partial q^i} - \Gamma_{jk}^i v^j v^k \frac{\partial}{\partial v^i}.$$

Now let τ_Q

$$\begin{aligned} \tau_Q : TQ &\rightarrow Q \\ v_q &\mapsto q \end{aligned}$$

denote the tangent bundle projection. Then, Eq. (18) written as a first order system evolving on TQ is

$$\dot{v}(t) = Z(v(t)) + u^a(t) \text{verlift}(Y_a(\tau_Q \circ v(t))) \quad (23)$$

where $v(t) \in TQ$. We now can define what it means for a mechanical system of the form in Eq. (18) to be $(\mathcal{U}, \bar{\mathcal{U}})$ -reducible to Eq. (22).

Definition A.4 Let ∇ be an affine connection on Q , and let \mathcal{U} and $\bar{\mathcal{U}}$ be two families of control functions. The system in Eq. (18) is $(\mathcal{U}, \bar{\mathcal{U}})$ -reducible to the system in Eq. (22) if the following two conditions hold:

- i) for each (\mathcal{U}, T) -solution (η, u) of the dynamic Eq. (18) with initial conditions $\eta(0)$ in the distribution D_{kin} , there exists a $(\bar{\mathcal{U}}, T)$ -solution (γ, \bar{u}) of the kinematic Eq. (22) with the property that $\gamma = \tau_Q \circ \eta$;
- ii) for each $(\bar{\mathcal{U}}, T)$ -solution (γ, \bar{u}) of the kinematic Eq. (22), there exists a (\mathcal{U}, T) -solution (η, u) of the dynamic Eq. (18) with the property that $\eta(t) = \gamma'(t)$ for almost every $t \in [0, T]$.

Condition i) says that for every solution of a dynamic system there must exist a kinematic solution that is the projection of the dynamic system. In the case of a vehicle, this corresponds to requiring that for every *trajectory* of the vehicle there exists a corresponding *path* that can be obtained from kinematic considerations alone. Condition ii) says that for every kinematic solution there must exist a dynamic solution that is equal to the kinematic solution coupled with its time derivative (so that it lies in TQ). This means that there must exist a dynamic solution for every feasible kinematic path.

Let $\chi^\infty(D)$ denote those C^∞ vector fields taking values in a distribution D . The following theorem states the local test for Eq. (18) to be $(\mathcal{U}_{\text{input}}, \mathcal{U}_{\text{input}})$ -reducible to Eq. (22).

Theorem A.1 (Lewis [6]) *Let ∇ be an affine connection, and let Y_1, \dots, Y_m and $X_1, \dots, X_{\bar{m}}$ be vector fields on a manifold Q . The control system in Eq. (18) is $(\mathcal{U}_{\text{input}}, \mathcal{U}_{\text{input}})$ -reducible to a system of the form in Eq. (22) if and only if the following two conditions hold:*

$$i) \text{span}_{\mathbb{R}}\{X_1(q), \dots, X_m(q)\} = \text{span}_{\mathbb{R}}\{Y_1(q), \dots, Y_{\bar{m}}(q)\}$$

for each $q \in Q$ (in particular, $\bar{m} = m$)

ii) $\langle X : Y \rangle \in \chi^\infty(D_{\text{dyn}})$ for every $X, Y \in \chi^\infty(D_{\text{dyn}})$ where $\langle \cdot, \cdot \rangle$ is the symmetric product of vector fields defined by

$$\langle X : Y \rangle = {}^G \nabla_X Y + {}^G \nabla_Y X \tag{24}$$

This theorem says that if the input distributions of both the kinematic system and the dynamic system are the same and the dynamic system is closed under symmetric products, then the system is kinematic. The following Lemma (from [18]) is a particularly useful result that we will use repeatedly in our analysis of the examples.

Lemma A.2 *Given a “constraint distribution” $D_{\text{con}} \subseteq TQ$ which annihilates the constraints $\{\omega_j\}$ and an input distribution D_{dyn} , if $D_{\text{dyn}} = D_{\text{con}}$ the mechanical system described by $\nabla_{\dot{q}} \dot{q} = u^\alpha Y_\alpha$ is $(\mathcal{U}_{\text{input}}, \mathcal{U}_{\text{input}})$ -reducible.*

This says that whenever when the constraint distribution is covered by the input distribution, $(\mathcal{U}, \bar{\mathcal{U}})$ reducibility of a multiple model mechanical system is guaranteed regardless of the metric G .